

Monitoring Rice Agriculture in the Sacramento Valley, USA With Multitemporal PALSAR and MODIS Imagery

Nathan Torbick, William A. Salas, Stephen Hagen, and Xiangming Xiao

Abstract—Rice agriculture is an important crop that influences land-atmosphere interactions and requires substantial resources for flood management. Multitemporal acquisition strategies provide an opportunity to improve rice mapping and monitoring of hydroperiod. The objectives of this study were to 1) delineate rice paddies with Phased Array L-band Synthetic Aperture Radar (PALSAR) fine-beam single/dual (FBS/D) mode measurements and 2) integrate multitemporal, ScanSAR Wide-Beam 1 (WB1)- and Moderate Resolution Imaging Spectroradiometer (MODIS)-observations for flood frequency mapping. Multitemporal and multiscale PALSAR and MODIS imagery were collected over the study region in the Sacramento Valley, California, USA. A decision-tree approach utilized multitemporal FBS (HH polarization) data to classify rice fields and WB1 measurements to assess paddy flood status. High temporal frequency MODIS products further characterized hydroperiod for each individual rice paddy using a relationship between the Enhanced Vegetation Index (EVI) and the Land Surface Water Index (LSWI). Validation found the PALSAR-derived rice paddy extent maps and hydroperiod products to possess very high overall accuracies (95% overall accuracy). Agreement between MODIS and PALSAR flood products was strong with agreement between 85–94% at four comparison dates. By using complementing products and the strengths of each instrument, image acquisition strategies and monitoring protocol can be enhanced. The results highlight how the integration of multitemporal PALSAR and MODIS can be used to generate valuable agro-ecological information products in an operational context.

Index Terms—Agriculture, ALOS PALSAR, hydroperiod, MODIS, multitemporal, rice.

I. INTRODUCTION

RICE is an important crop globally that influences food security and the Earth system. Rice is the predominant food staple in many regions with approximately 650 million tons (milled basis) in production annually. This requires large

resources through irrigation management and hydroperiod control. Rice hydroperiod is the flood frequency and duration of flooding for a paddy. The role of rice hydroperiod is poorly understood and potentially plays a large role in greenhouse gas emissions [1]–[4]. Methane (CH_4) is one of the largest contributors to human-induced atmospheric change, second behind carbon dioxide. CH_4 from rice accounts for 20% of global sources [5], [6] with irrigated rice accounting for 80% of rice CH_4 emissions [7]. In order to more thoroughly monitor rice agriculture and assess management impacts improved operational information on rice extent and hydroperiod is needed.

The use of high temporal frequency MODIS imagery for rice mapping has recently been exploited as a monitoring tool. Primary advantages of MODIS measurements are the frequent repeat intervals of the satellite platform. The MODIS Science Team provides a suite of products including surface reflectance with bands that are sensitive to water and vegetation. Xiao *et al.* [8] developed an approach based on 8-day MODIS indexes to map rice and agro-ecological attributes. The algorithm, based on multitemporal MODIS, has been successfully employed in regions in South and Southeast Asia for mapping rice over large areas [9]. Sakamoto *et al.* [10] also found multitemporal MODIS useful to map rice and assess flood patterns in the Mekong Delta.

A number of recent studies have also highlighted the advantages of multitemporal L-band Synthetic Aperture Radar (SAR) for monitoring rice agriculture [5], [11]–[13]. The primary advantage of SAR data is its ability to penetrate canopies and its sensitivity to vegetation structure, water content, and biomass independent of weather conditions. L-band SAR has been shown to be particularly sensitive to aquatic above ground biomass [12], [14]. Utilizing multitemporal L-band SAR enables capturing backscatter dynamics which is useful for monitoring biogeophysical attributes such as hydroperiod. For example, Rosenqvist *et al.* [15] and Costa *et al.* [16] were able to model hydroperiod dynamics using multitemporal L-band SAR data with *in situ* river gauge measurements to characterize portions of the Amazon floodplain.

This study takes advantage of both sensor strengths, that is L-band SAR's radiometric sensitivity to rice biogeophysical attributes and the high temporal frequency of MODIS, to identify rice paddies and monitor rice hydroperiod. The objectives of this study were to 1) delineate rice paddies with PALSAR FBS (HH) measurements and 2) integrate multitemporal, ScanSAR Wide-Beam 1 (WB1)- and MODIS- observations for flood frequency mapping. The study was carried out in an economically

Manuscript received May 28, 2009; revised February 10, 2010 and June 09, 2010; accepted November 03, 2010. Date of publication December 10, 2010; date of current version May 20, 2011. This work was supported in part by the JAXA Kyoto & Carbon Initiative, the NASA LCLUC program (#NNX08AL16G), and the Natural Resource Conservation Service. ALOS PALSAR data were provided by JAXA EORC and Terra/Aqua MODIS data were provided by NASA.

N. Torbick, W. A. Salas, and S. Hagen are with Applied Geosolutions, Durham, NH 03857 USA (e-mail: torbick@agsemail.com).

X. Xiao is with the Department of Botany and Microbiology and Center for Spatial Analysis, University of Oklahoma, Norman, OK 73019 USA.

Color versions of one or more of the figures in this paper are available online at <http://ieeexplore.ieee.org>.

Digital Object Identifier 10.1109/JSTARS.2010.2091493

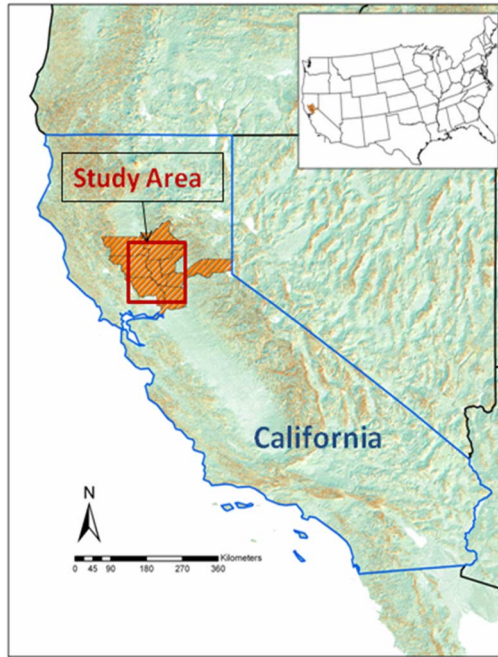


Fig. 1. Study area (red box) in the northern Sacramento Valley, California, USA. Portions of eight counties (orange polygons) contain 95% of the rice grown in the state.

important rice growing region in the Sacramento Valley, California, USA.

II. METHODS

The methodological approach was divided into sectional formats to circumvent repetitive presentation. Three following methodological sections describe the *A. Study area*, *B. Satellite data and classification*, and *C. Field campaign and reference data*.

A. Study Area

The study area is a large, commercially important rice growing region located in the northern Sacramento Valley, California, USA (centered ~ 121.825 W, 39.20 N). Approximately 95% of rice produced in California is cultivated in this region with nearly half a billion dollars generated annually [17]. California is the largest producer of short and medium grain japonica rice in the USA. The study area includes portions of eight counties that have substantial rice paddy agriculture including: Butte, Colusa, Glenn, Placer, Sacramento, Sutter, Yolo, and Yuba (Fig. 1). Other dominant land use land cover (LULC) classes in the region include natural vegetation (33%), deciduous fruits and nuts (20%), sub/urban (10%), field crops (10%), and pasture (5%) among other covers. Average temperatures are 6.1 and 22.8 degrees C in January and July, respectively. Annual precipitation in Sacramento averages 43.7 cm; whereas, annual precipitation in Redding in the northern part of the Sacramento Valley averages 103.9 cm. Intensive irrigation and agricultural management occurs in the area.

B. Satellite Data and Classification

The Advanced Land Observation Satellite (ALOS) orbits with the PALSAR instrument in a Sun-synchronous pattern at

an altitude of 691.65 km and an inclination of 98.16° . PALSAR is a fully polarimetric instrument, operating in fine-beam mode with single polarization (HH or VV), dual polarization (HH + HV or VV + VH), or full polarimetry (HH + HV + VH + VV). It also features wide-swath ScanSAR mode with single polarization (HH or VV). The center frequency is 1270 MHz (23.6 cm), with a 28 MHz bandwidth in fine beam single polarization mode, and 14 MHz in the dual-pole, quad-pole and ScanSAR modes. The off-nadir angle is variable between 9.9° and 50.8° (at midswath), corresponding to a $7.9 - 60.0^\circ$ incidence angle range. In 5-beam ScanSAR mode the incidence angle range varies from 18.0° to 43.0° . Ground resolutions depend on mode and range from FBS at 6.25 m pixel spacing with 30/70 km swaths to 100 m pixel spacing at 350 km ScanSAR swaths all in the right look direction. Absolute radiometric accuracy is < 1.5 dB between orbits [18].

As part of the Japan Aerospace Exploration Agency (JAXA) Kyoto & Carbon Initiative, a PALSAR acquisition strategy has been developed with a goal of having spatially and temporally consistent data at continental scales with adequate revisit frequency and timing to enable the development of large-area products. The wetlands science team contributed to the development of the PALSAR acquisition strategy that includes ScanSAR data acquisitions of major wetlands regions every 46 days for regional mapping and characterization of aquatic ecosystems. Adjacent acquisitions overlap 50%, so effectively there are 2 acquisitions every 46 days continuously starting from October 2006.

PALSAR imagery was previewed through the Alos User Interface Gateway (AUIG 3.0) operated by JAXA. At the JAXA Earth Observation Center, FBS/D data were resampled using cubic convolution and ScanSAR using a bilinear scheme to project into the Universal Transverse Mercator (UTM) Zone 10 North coordinate system. FBS/D pixel spacing included both 6.25 and 12.5 m resolutions with a typical footprint covering approximately 80×75 km (~ 6000 km²). While some imagery was collected in FBD mode, in this study only HH polarization was used in analysis. Only HH was used because of PALSAR's effort for operational acquisitions for longer-term monitoring frameworks. In addition, the double bounce pattern between rice and HH has been well-established and the observations covered the entire study area during the needed phenological period. ScanSAR was obtained as orthorectified (ORT), ground range (GRD) imagery at 100 m pixel spacing covering approximately 420×440 km (~ 184800 km²). The target temporal period was the 2007 rice season.

Twenty five (25) FBS/D images during the rice growing season were utilized (Table I) for comprehensive coverage of the study area twice (wet/planting and dry/harvest). The schedule from flood-up to rice harvest is approximately between Day of Year (DOY) 160–275. Twelve (12) scenes were acquired during the flood season (\sim DOY160) and thirteen (13) scenes during the harvest season (\sim DOY275). One scene during the harvest period was a small footprint so an additional fine-beam image was required. This approach provided two seamless FBS coverages of the entire (“wall-to-wall”) northern Sacramento Valley. In order to characterize the off season (rice fields dormant) flood cycles four ScanSAR WB1 images were collect on 12/5/2006, 1/20/2009, 3/7/2007, and 4/17/2007.

TABLE I
PALSAR IMAGES USED TO OBTAIN COMPLETE MULTI-TEMPORAL FBS
COVERAGE OF THE STUDY AREA AND MULTI-TEMPORAL SCANSAR AND
MODIS IMAGERY TO CHARACTERIZE HYDROPERIOD. ORBITS INCLUDE BOTH
DESCENDING AND ASCENDING

Obs	Res (m)	Temporal	No. of Scenes
FBS	12.5	DOY 160 & 275	25
WB1	100	winter season	4
MODIS	500	every 8 days	46/yr

These dates were used to characterize a ‘typical’ winter flood cycle in the region and develop an operational approach. The ScanSAR overpass on 1/20/2009 was concordant with a field campaign to assess product accuracy. With large temporal gaps between SAR overpasses present, we integrated the high temporal frequency optical data to create a seamless hydroperiod monitoring throughout the year. We conducted an accuracy assessment by comparing four corresponding PALSAR and MODIS time periods as well as using ground truth (1/20/2009) of both PALSAR and MODIS flood products.

All SAR data used were HH polarization. Imagery was obtained as unsigned 16-bit processed level 1.5 originally in CEOS format. Level 1.5 is defined by generic radiometric and geometric corrections performed according to specified map projections after performing range and multi-look azimuth compressions [19]. Additional radiometric adjustments were executed following the cosine of the zenith angle approach [20] to correct for viewing geometry affects; no further local incident angle corrections were needed as the study area and classification target (i.e., rice paddies) are extremely flat and fields in this region are large and continuous. Scripts performed multiple tasks and transformed data into geotiffs of Digital Number (DN) and backscatter coefficients (γ and σ^0) as well as creating metadata files:

$$\sigma^0 = 10 * \log_{10}(\text{DN}^2) + \text{Calibration Factor.} \quad (1)$$

Once pre-processing was complete the PALSAR imagery was ingested into the second processing stream (Fig. 2). A simple decision-tree framework based on thresholding FBS values was used to identify rice paddies by capturing the characteristics of flooded areas and dynamic range representing rice growth. Pixel-based statistics (minimum, maximum, range) were extracted from the multitemporal FBS imagery to threshold and generate a rice extent map (ie, rice versus non-rice). Threshold values were obtained from fields identified as rice paddies in the FBS/D imagery. Next, a majority filter was applied to eliminate isolated pixels randomly distributed across the landscape. A similar decision-tree procedure was applied to the ScanSAR imagery to identify water. For each rice paddy delineated from FBS PALSAR, hydroperiod status (flooded versus nonflooded) was extracted from the multitemporal ScanSAR measurements classified for water and nonwater pixels. Summarizing, this processing stream created a rice extent map and multitemporal hydroperiod maps for each rice paddy.

The MODIS instrument is carried onboard the Terra and Aqua satellite platforms which have been orbiting since

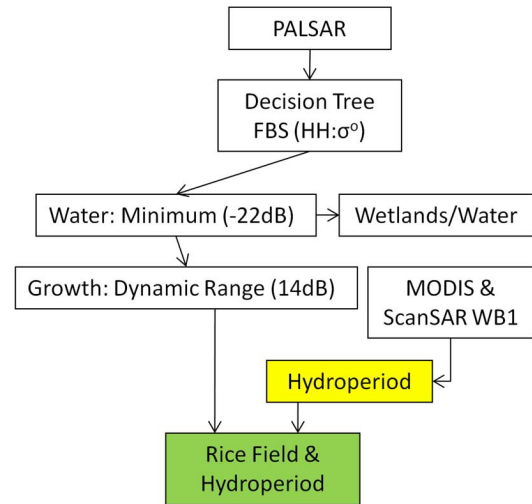


Fig. 2. Schematic detailing the main decision tree elements for monitoring rice agriculture. The classifier thresholds FBS observations to delineate rice paddies. ScanSAR and MODIS data characterize hydroperiod.

1999 and 2002, respectively. Terra (descending) and Aqua (ascending) are in a Sun-synchronous, circular orbit at an altitude of 705 km. The instrument collects measurements in 36 spectral bands every 1–2 days at spatial resolutions of 250 m–1 km. A single MODIS tile covers a 1200 × 1200 km area in Sinusoidal projection. MODIS products are freely available from the Land Processes Distributed Active Archive Center (LPDAAC) through the Warehouse Inventory Search Tool (WIST) in HDF-EOS format.

MODIS MCD43A4 collection five products are nadir-adjusted, 500 m surface reflectance corrected using bidirectional reflectance distribution function (BRDF) and atmospheric models [21], [22]. The MCD43A4 algorithm uses a 16-day moving window to generate products at 8-day intervals using observations from both the Terra and Aqua platforms. This provided 46 composites annually for each rice paddy. Composites utilize optimal pixels by eliminating contaminated pixels identified through a quality control flagging process. We used the high temporal frequency MODIS to temporally gap fill SAR observations.

Preprocessing reprojected data into a common projection and used MODIS QAQC (MCD43A2) flags to identify potentially contaminated pixels. Contaminated pixels were eliminated from analyses. To identify flooded rice paddies a multistep process was executed. For each PALSAR FBS HH classified rice paddy, a filter was applied to high frequency MODIS indices. The filter used a relationship between the Land Surface Water Index (LSWI) [(2)] and the Enhanced Vegetation Index (EVI) [(3)].

$$LSWI = \frac{\rho_{nir} - \rho_{swir}}{\rho_{nir} + \rho_{swir}} \quad (2)$$

$$EVI = 2.5 \times \frac{\rho_{nir} - \rho_{red}}{\rho_{nir} + 6\rho_{red} - 7.5\rho_{blue} + 1} \quad (3)$$

$$\text{MODIS Flood} = \text{LSWI} + 0.05 > \text{EVI} \quad (4)$$

EVI builds on previous indexes that measure vegetative surface conditions by incorporating information from the blue (MODIS blue band = 459–479 nm) band’s sensitivity to the

atmosphere and coefficients adjusting for soil and background effects [23]. LSWI utilizes shortwave infrared's (SWIR) sensitivity to moisture and has been used to assess ecological conditions and flood dynamics previously [10], [24]. A filter constrained the observation period to include flooding through rice development to harvest. A temporary inversion of the vegetation indices, where LSWI either approaches or is higher than EVI values, signals flooding in paddy rice fields. To slightly relax the simple threshold assumption an adjustment factor is included [9]. In this study flood characterization was determined using the relationship between LSWI and EVI [(4)]. This algorithm has been successfully implemented in China [8] and South and Southeast Asia [9] to map rice paddies.

C. Field Campaign & Reference Data

An accuracy assessment was carried out to assess the two primary rice information products: the rice paddy extent map and the hydroperiod maps. FBS rice paddy classifications and ScanSAR hydroperiod products were assessed for overall accuracy and misclassification patterns. A series of error matrices were constructed using field-level data and high resolution color photography as reference. Orthorectified National Agriculture Imagery Program (NAIP) mosaics were utilized as ground control reference for the rice extent map. NAIP data collection occurred at Day Of Year (DOY) 215 and 253 which is during the rice growing period in the study area. These true-color, 1-meter, digital photos are available through the United States Department of Agriculture (USDA) Geospatial Data Gateway. Data are compressed in Mr.Sid format with a horizontal accuracy within 3 meters. Mosaics are tiled using a $3.75' \times 3.75'$ quarter quads formatted to the UTM projection system using North American Datum 1983 (NAD83).

For the FBS rice extent maps a stratified random sampling scheme was utilized to insure statistical sampling rigor followed well-established accuracy protocol [25]. No training sites were included in the accuracy assessment. The validation scheme identified the maximum classified proportion to generate a specified sample size ($n = 475$). A stratified random distribution with 250 rice points separated with a minimum distance of 300 m was applied to consider landscape context and patch size (i.e., rice field). A second set of stratified random points were distributed among pixels classified as non-rice using ancillary data from the Department of Water Resources (DWR) in California. Together these assessment data points provided 475 unique, statistically rigorous validation points. The accuracy points were checked using a two-tiered approach. First, all points were compared against DWR LULC data and second all points were verified against the NAIP imagery.

For the ScanSAR WB1 hydroperiod products, a near-simultaneous field campaign was performed to assess the accuracy of the flood products in the study region. The ALOS overpass date was January 20, 2009 (DOY20) with the field campaign four days following the overpass. From the binary FBS rice maps two large and dense paddy clusters were chosen as focus areas for the winter flood assessment. The clusters were approximately 50 km north of the City of Sacramento and 25 km west of the City of Oroville. Ground truth data were collected using a GPS-enabled camera at approximately 1000 m equal intervals following



Fig. 3. Two GPS-enabled camera ground truth points showing correct classifications of flooded rice paddies identified from multitemporal FBS and ScanSAR imagery.

the road network. A windshield survey (“drive-by transects”) was carried out and points were systematically collected within the two pre-selected clusters. GPS photos were collected perpendicular to the road direction using the stratified approach. A total of 130 points (Fig. 3) were collected for the second portion of the assessment designed to validate the hydroperiod products.

III. RESULTS AND DISCUSSION

A. Mapping Rice in the Sacramento Valley, USA

The FBS data were used to delineate rice paddies according to the decision tree framework (i.e., threshold values) and overpass dates. The decision-tree identified nearly 155,000 hectares of rice paddies undergoing cultivation during the temporal FBS overpasses with an average patch size of 47 hectares. The FBS temporal windows (DOY of overpass) had a target of early and late development of the single rice crop system. In this region it is possible that rice fields are planted with off season cover crops for nutrient accumulation or managements allow native vegetation to thrive to create habitat for migratory waterfowl. These factors created challenges and were thus considered when creating and defining the rules within the decision-tree framework.

Threshold values based off empirical rice growth data and image statistics collected from training fields were both utilized as threshold rules (Table II). A set of trial runs were carried out evaluating the results of varying the thresholds values. Qualitative inspection found too strict (i.e., small threshold for dynamic range) thresholds resulted in a patchy classification with ample

TABLE II
THREE EXAMPLE RICE TRAINING FIELDS AND ASSOCIATED IMAGE STATISTICS
FOR GENERATING RICE THRESHOLD VALUES FROM FLOODED, PEAK
MATURATION, AND RANGE. HH VALUES ARE DISPLAYED IN σ^0

	Field 1	Field 2	Field 3
	Mean	Mean	Mean
Rice season (min)	-22.23	-22.90	-22.67
Rice season (max)	-10.08	-6.61	-9.52
Rice season (range)	12.15	16.29	13.15

omission error; while, overly eased rules (i.e., high minimum value for water pixels and large threshold for dynamic range) resulted in a saturated classification with high commission errors present.

For a quantitative and application approach, image statistics generated from training polygons were identified as the optimal approach to define threshold rules. A set of rice training fields (comprised of $\sim 40,000$ known rice pixels) provided minimum, maximum, and dynamic range values for the decision tree threshold values. Average minimum, maximum, and range (σ^0) used were -22.6 , -8.7 , and 13.9 , respectively. This approach provided a straight forward quantitative and operational approach to develop the decision tree rules with little *a priori* data; however, we emphasize that threshold values based on the empirical rice growth model also provided acceptable rice classifications. Using the empirical model approach also allows for automated mapping in an operational context with no *a priori* data. Empirical values were obtained from Inoue *et al.* [12] and qualitatively results were comparable to the products generated using threshold values. However, we note that we did not quantitatively compare threshold results to empirical model results in this project as that was not an objective.

Accuracy assessment of the final decision tree was carried out using NAIP reference data. The FBS rice paddy classification had an overall accuracy of 96% ($449/469 = 0.957$). Twenty points were interpreted as misclassified giving an overall omission error of 0.043. Kappa statistics had a khat value of 0.91 with a variance and z-score value of 0.00037 and 47.75, respectively with a p-value significance of <0.00001 .

PALSAR FBS measurements obtained during key rice phenology periods contributed to the very high accuracy of the rice extent maps. We further highlight that the landscape in the region lends itself well to classification. In general the fields are large and continuous, the landscape is extremely flat and well developed, and the study area is a commercial rice region therefore dominated by a few land uses/covers.

The misclassified points were distributed among five categories of errors. The majority of these errors were related to temporal challenges ($n = 12$). This means that the threshold values used in the decision-tree classifier to define the rice paddy extent eliminated a potential rice field due to shifts in flood cycles, harvest date, and/or overpass timing. Three errors were related to spatial problems where a point fell just outside a rice field or classified rice pixel. Wetland riparian areas caused three misclassifications. These areas had seasonally standing water and

dynamic range similar to the thresholding values of paddies used in the decision tree. One misclassification was from a grain crop and the remaining misclassification was unknown and could not be determined as rice.

B. Monitoring Rice Hydroperiod

A similar approach to evaluating threshold values was carried out for the ScanSAR flood maps. With water as the target class, little difference was observed between known/empirical data and image training statistics (i.e., identify average minimum and SD). The MODIS flood maps generated a binary outcome derived from $LSWI + 0.05 > EVI$ to determine flood status. The FBS rice map was used as a mask to extract hydroperiod (flooded or not flooded) derived from the ScanSAR and MODIS measurements. With the FBS rice map, each rice paddy obtained its unique hydroperiod pattern. With ScanSAR at 100 m and MODIS at 500 m, some mixed pixels were present in an individual rice paddy mapped from 12.5 m SAR imagery. Within the decision-tree if any rice field had at least 25% area characterized as flooded from ScanSAR, then that rice paddy was considered as flooded. With the landscape primarily represented by large, commercial scale rice paddies (average paddy ~ 47 hectares, range 1–1132 ha) this was not an issue for ScanSAR. If a rice paddy detected part of a MODIS flooded pixel then the rice field was considered flooded for that time period.

Fieldwork was performed to evaluate accuracy of the ScanSAR flood products. The ALOS overpass date was January 20, 2009 and ground-truthing occurred within four days. Visual interpretation of the ground truth photos resulted in an overall accuracy of 96% (124/129). Approximately half of the points were flooded. One point was thrown out due to error. Due to the size of MODIS pixels (~ 500 m), MODIS flood products were evaluated by comparing them against four different ScanSAR flood maps. The comparison dates used the nearest MODIS 8-day interval. Therefore, ALOS overpass dates December 5, 2006, March 7 2007, April 17, 2007, and January 20, 2009 corresponded to MODIS DOY 2006339, 2007066, 2007107, and 2009020, respectively.

Generally, the flood products between the two sensors had strong agreement (Table III). Two by two contingency tables (i.e., binary flood versus not flooded error matrices) resulted in agreements of 84–95%. The DOY 2006339 comparison had the most MODIS fill values (i.e., no data) with 28% of rice paddies containing portions of no fill pixels. The DOY 2009020 comparison had 251 rice paddies (8%) containing portions of no fill MODIS pixels. No fill values were filtered for the final comparisons resulting in a varying number of paddies compared at each interval. To assess the influence landscape configuration and pixel size, all rice paddies under 50 hectares were withheld to assess accuracy of only larger fields. No statistically significant difference was found related to the size of paddies and accuracy in this study area.

While a small portion of MODIS tended to have no data values, the high frequency intervals allow more precise hydroperiod characterization compared to the PALSAR imagery alone (Fig. 4). The MODIS flood products can be used to refine model parameterization where finer-time intervals are desired and can influence GHG model output [3]. In this study

TABLE III
AGREEMENT BETWEEN PALSAR AND MODIS FLOOD PRODUCTS USING THE OPERATIONAL ALGORITHMS FOR THE FOUR COMPARISON TIME INTERVALS IN THE STUDY REGION (NF = not flooded, F = flooded)

		PALSAR	
		NF	F
2006339	MODIS NF	2174	101
	MODIS F	307	174
Agreement: 85.2%			
		PALSAR	
		NF	F
2007066	MODIS NF	2975	177
	MODIS F	0	0
Agreement: 94.4%			
		PALSAR	
		NF	F
2007107	MODIS NF	2696	321
	MODIS F	27	108
Agreement: 89.0%			
		PALSAR	
		NF	F
2009020	MODIS NF	2292	128
	MODIS F	328	210
Agreement: 84.6%			

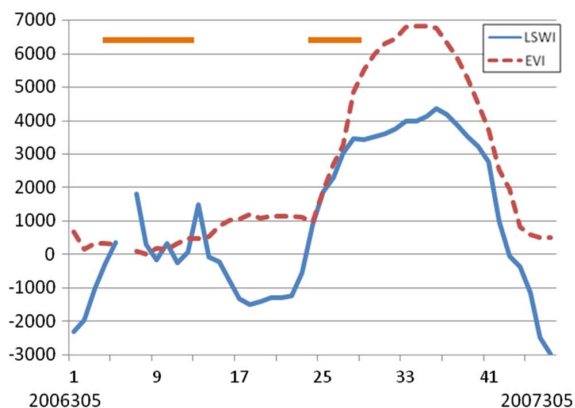


Fig. 4. MODIS 8-day (x axis interval) LSWI (blue line) and EVI (red dashed line) rescaled and plotted over time for rice paddy #574 (83 hectares) for one year starting November 1, 2006. Orange line on graph marks flooded periods for winter flood and summer flood/planting.

a straightforward thresholding approach was carried out. Potentially, higher accuracy for any time period can be achieved; however, this would require altering the algorithms (threshold values) thus not truly operational. With integrated PALSAR and MODIS products a more thorough monitoring strategy was achieved for each individual rice paddy. When working in a region with little to no *a priori* information, MODIS can be used to define temporal windows in which PALSAR overpass data is well-suited.

Summarizing the flood products, approximately half of all paddies (74,292 hectares) were flooded during the December

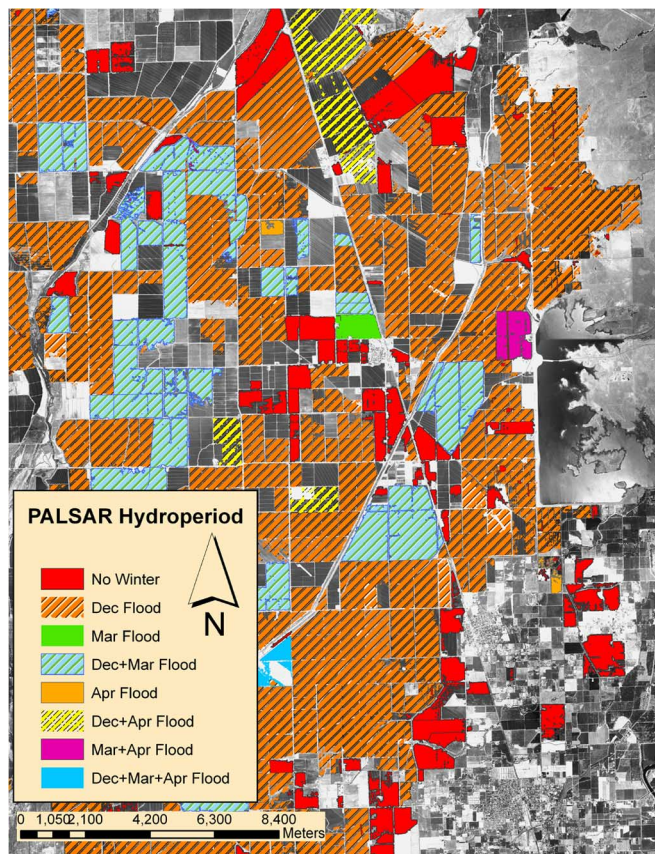


Fig. 5. Map of rice paddies and rice paddy hydroperiod generated from FBS/D (HH: 12.5 m) and ScanSAR WB1 (HH: 100 m), respectively. Approximately 75,000 hectares of rice paddies were cultivated in the rice growing season of 2007 in the Sacramento Valley, California, USA. Of these, approximately half (47%) were identified as flooded only during the December overpass.

overpass. The ScanSAR images from 12/5/2006, 1/20/2009, 3/7/2007, and 4/17/2007 were used to represent a typical winter flooding regime from PALSAR observations. Not only is binary information on flood status valuable, but length of flood cycle is important as it impacts biogeochemical interactions. This is when the MODIS 8-day observations can be used to gap fill SAR observations. About one-third of the rice fields identified (~42,341 hectares) underwent no flooding conditions according to the PALSAR temporal overpass windows observed in this study. Over 5,000 hectares, or about 3.5% of identified fields, were flooded throughout the entire off season. It is likely these fields are utilized as migratory waterfowl habitat or carrying out managements for residue decomposition. The hydroperiod maps show the heterogeneous pattern of flood cycles across the region (Fig. 5). Approximately 71% of all rice paddies were flooded at least once during the winter time period before the next seeding event.

IV. CONCLUSIONS

The operational approach executed in this study mapped rice extent and rice hydroperiod with a relatively strong degree of accuracy for the Sacramento Valley, USA. Using the strengths of multitemporal PALSAR and MODIS a more thorough and integrated approach allows for systematic monitoring of agro-ecological attributes. These results coupled with the overpass frequency of MODIS and the acquisition strategy being develop for

PALSAR by JAXA, indicate that large-area mapping and monitoring is achievable. These systematic products can be used to improve water resources management, assess GHG emissions, and coordinating waterfowl habitat. Future objectives will focus on assessing longer-term hydroperiod cycles.

REFERENCES

- [1] J. Johnson, A. Franzluebbers, S. Weyers, and D. Reicosk, "Agricultural opportunities to mitigate greenhouse gas emissions," *Environmental Pollution*, vol. 150, pp. 107–124, 2007.
- [2] C. Li, S. Frolking, X. Xiao, B. Moore, S. Boles, J. Qiu, Y. Huang, W. Salas, and R. Sass, "Modeling impacts of farming management alternatives on CO₂, CH₄, and N₂O emissions: A case study for water management of rice agriculture in China," *Global Biogeochemical Cycles*, vol. 19, 2005, doi 10.1029/2004GB002341.
- [3] W. Salas, S. Boles, C. Li, J. Yeluripati, X. Xiao, S. Frolking, and P. Green, "Mapping and modeling of greenhouse gas emissions from rice paddies with satellite radar observations and the DNDC biogeochemical model," *Aquatic Conservation: Marine and Freshwater Ecosystems*, vol. 17, pp. 319–329, 2007.
- [4] Y. Zhang, C. Wang, J. Wu, J. Qi, and W. Salas, "Mapping paddy rice with multi-temporal ALOS PALSAR imagery in Southeast China," *Int. J. Remote Sens.*, pp. 6301–6315, 2009.
- [5] Intergovernmental Panel on Climate Change (IPCC), "Climate Change: The Supplementary Report to the IPCC Scientific Assessment," Cambridge Univ. Press, New York, NY, 1992.
- [6] K. Lassey, "Livestock methane emissions: From the individual grazing animal through national inventories to the global methane cycle," *Agricultural and Forest Meteorology*, vol. 142, pp. 120–132, 2007.
- [7] R. Wassmann, H. U. Neue, R. S. Lantin, K. Makarim, N. Chareonsilp, L. V. Buendia, and H. Rennenberg, "Characterization of methane emissions from rice fields in Asia. II. Differences among irrigated, rainfed, and deepwater rice," *Nutrient Cycling in Agroecosystems*, vol. 58, pp. 13–22, 2000.
- [8] X. M. Xiao, S. Boles, J. Y. Liu, D. F. Zhuang, S. Frolking, and C. Li *et al.*, "Mapping paddy rice agriculture in southern China using multi-temporal MODIS images," *Remote Sens. Environ.*, vol. 95, pp. 480–492, 2005.
- [9] X. Xiao, S. Boles, S. Frolking, C. Li, J. Badu, W. Salas, and B. Moore, "Mapping paddy rice agriculture in South and Southeast Asia using multi-temporal MODIS images," *Remote Sens. Environ.*, vol. 100, pp. 95–113, 2006.
- [10] T. Sakamoto, M. Yokozawa, H. Toritani, M. Shibayama, N. Ishitsuka, and H. Ohno, "Spatio-temporal distribution of rice phenology and cropping systems in the Mekong Delta with special reference to the seasonal water flow of the Mekong and Bassac rivers," *Remote Sens. Environ.*, vol. 100, pp. 1–16, 2008.
- [11] N. Torbick, X. Xiao, and W. Salas, "Mapping rice agriculture with ALOS PALSAR," presented at the NASA Science Team Meeting, Washington DC, Apr. 2009.
- [12] Y. Inoue, T. Kurosu, H. Aeno, S. Uratsuka, T. Kozu, K. DabrowskaZielinska, and J. Qi, "Season-long daily measurements of multifrequency (*Ka*, *Ku*, *X*, *C*, and *L*) and full-polarization backscatter signatures over paddy rice field and their relationship with biological variables," *Remote Sens. Environ.*, vol. 81, pp. 194–204, 2002.
- [13] C. Wang, J. Wu, Y. Zhang, G. Pan, J. Qi, and W. Salas, "Characterizing L-band scattering of paddy rice in southeast China with radiative transfer model and multi-temporal ALOS/PALSAR imagery," *IEEE Trans. Geosci. Remote Sens.*, vol. 47, pp. 988–998, 2009.
- [14] E. Novo, M. Costa, J. Mantovani, and I. Lima, "Relationship between macrophyte stand variables and radar backscatter at L and C band, Tukurui reservoir, Brazil," *Int. J. Remote Sens.*, vol. 23, pp. 1241–1260, 2002.
- [15] A. Rosenqvist, B. Forsberg, T. Pimentel, Y. Rauste, and J. Richey, "The use of spaceborne radar data to model inundation patterns and trace gas emissions in the central Amazon floodplain," *Int. J. Remote Sens.*, vol. 23, pp. 1303–1328, 2002.
- [16] M. Costa, "Use of SAR satellites for mapping zonation of vegetation communities in the Amazon flood-plain," *Int. J. Remote Sens.*, vol. 25, pp. 1817–1835, 2004.
- [17] W. Wong, "Comparative emission of methane from different rice straw management practise in California- A statewide perspective," *J. Sustainable Agriculture*, vol. 22, pp. 79–91, 2003.
- [18] A. Rosenqvist, S. Shimada, and M. Watanbe, "ALOS PALSAR: Technical outline and mission concepts," presented at the 4th Int. Symp. Retrieval of Bio- and Geophysical Parameters From SAR Data for Land Applications, Innsbruck, Austria, Nov. 16–19, 2004.
- [19] PALSAR Reference Guide 2006, Earth Remote Sensing Data Analysis Center (ERSDAC), Technical Develop II. PALSAR Data Service Section, p. 57.
- [20] S. Liang, *Topographic Correction Methods: Quantitative Remote Sensing of Land Surfaces*. New York: Wiley, 2005, ch. 7, 10.1002/047172372X.
- [21] C. B. Schaaf, F. Gao, A. H. Strahler, W. Lucht, X. Li, and T. Tsang, "First standard BRDF, albedo and nadir reflectance products from MODIS," *Remote Sens. Environ.*, vol. 83, pp. 135–148, 2002.
- [22] E. Vermot, N. El Saleous, and C. Justice, "Atmospheric correction of the MODIS data in the visible to middle infrared: First results," *Remote Sens. Environ.*, vol. 83, pp. 97–111, 2002.
- [23] A. Huete, K. Didan, T. Miura, and E. Rodriguez, "Overview of the radiometric and biophysical performance of the MODIS vegetation indices," *Remote Sens. Environ.*, vol. 83, pp. 195–213, 2002.
- [24] X. Xiao, S. Boles, S. Frolking, W. Salas, B. Moore, and C. Li *et al.*, "Observation of flooding and rice transplanting of paddy rice fields at the site to landscape scales in China using VEGETATION sensor data," *Int. J. Remote Sens.*, vol. 23, pp. 3009–3022, 2002.
- [25] R. Congalton and K. Green, *Assessing the Accuracy of Remotely Sensed Data: Principles and Practices*. Boca Raton, FL: CRC/Lewis Press, 1999, p. 137.

Nathan Torbick is a Research Scientist at Applied Geosolutions, LLC, Durham, NH. Dr. Torbick joined AGS after completing his graduate work at the Center for Global Change and Earth Observation at Michigan State University. He received the B.S. and M.S. degrees in environmental science and geography from the University of New Hampshire and the University of Toledo, respectively. His research foci are human–environment interactions, aquatic ecosystem remote sensing, and decision support systems.

William A. Salas is President and Chief Scientist of Applied Geosolutions, LLC, Durham, NH. Dr. Salas has degrees in mathematics, forestry, and natural resources from the Universities of Vermont and the University of New Hampshire, respectively. He is a member of the Scientific Advisory Panel for the ALOS Kyoto and Carbon Initiative under the auspices of the Japanese Space Agency. His research interests are centered around on building tools for GHG emission inventories, developing process models for estimating air emissions from animal feeding operations and developing web-based decision support systems for agricultural and rangeland management through the integration of GIS, remote sensing, and the DNDC biogeochemical model.

Stephen Hagen joined Applied Geosolutions, Durham, NH, in 2006 after completing his Ph.D. in earth systems science at the University of New Hampshire. Dr. Hagen's research interests center on the use of models and data mining techniques to extract information about the land surface and physical processes from large geospatial data sets, particularly remote sensing data. A key component of this research includes the robust estimation of uncertainty involved in modeling physical systems. Dr. Hagen received the B.S. and M.S. degrees in systems engineering from the University of Virginia, Charlottesville, in the late 1990s.

Xiangming Xiao received the Bachelor's degree in biology from Xiamen University, China, in 1982, the Master's degree in plant ecology from the Institute of Botany, Chinese Academy of Science and University of Science and Technology, China, in 1987, a UNEP/UNESCO Diploma of Environmental Management and Protection from the University of Technology, Dresden, Germany, in 1988, and the Ph.D. degree in ecosystem science from Colorado State University in 1994.

Dr. Xiao recently began a new position at the University of Oklahoma after working at the Complex Systems Research Center at the University of New Hampshire. His research interests span a wide range of biological science, geoscience and health science, including climate change, land use and land cover change, global carbon cycle, remote sensing, and epidemiology and ecology of infectious diseases.